Large scale drag representation in simulations of two-dimensional turbulence

Semion Sukoriansky
Department of Mechanical Engineering, Ben-Gurion University of the Negev, Beer-Sheva 84105, Israel

Boris Galperin
Department of Marine Science, University of South Florida, St. Petersburg, Florida 33701

Alexei Chekhlov
Program in Applied and Computational Mathematics, Princeton University, Princeton, New Jersey 08544, and Paribas Corporation, 787 Seventh Avenue, New York, New York 10019

(Received 8 May 1998; accepted 8 June 1999)

Numerical simulations of isotropic, homogeneous, forced and dissipative two-dimensional (2D) turbulence in the energy transfer subrange are complicated by the inverse cascade that continuously propagates energy to the large scale modes. To avoid energy condensation in the lowest modes, an energy sink, or a large scale drag is usually introduced. With a few exceptions, simulations with different formulations of the large scale drag reveal the development of strong coherent vortices and steepening of energy and enstrophy spectra that lead to erosion and eventual destruction of Kolmogorov–Batchelor–Kraichnan (KBK) statistical laws. Being attributed to the intrinsic anomalous fluctuations independent of the large scale drag formulation, these coherent vortices have prompted conjectures that KBK 2D turbulence in the energy subrange is irreproducible in long term simulations. Here, we advance a different point of view, according to which the emergence of coherent vortices is triggered by the inverse energy cascade distortion directly attributable to the choice of a large scale drag formulation. We subdivide the computational modes into explicit and implicit, or supergrid scale (SPGS), which are the few lowest wave numbers modes that adhere to KBK statistics. Then, we introduce a new concept of the large scale drag—rather than being an energy sink, it accounts for the energy and enstrophy exchange between the explicit and SPGS modes. The new SPGS parameterization was used in both direct numerical simulations (DNS) and large eddy simulations (LES) in a doubly periodic box setting. It was found that the new technique enables both DNS and LES to reach a steady state preserved for many large scale eddy turnover times. For the entire time of integration, the flow field remained structureless and in good agreement with the KBK statistical laws. We conclude that homogeneous, isotropic, forced, dissipative 2D turbulence in the energy subrange is statistically stable, does not produce coherent structures, and obeys the KBK statistical laws for as long as its inverse energy cascade remains undisturbed. The proposed new technique of computing the intermediate modes while the statistics of the largest scales is known may find a wide range of applications. [S1070-6631(99)00110-5]

I. INTRODUCTION

One of the most distinctive features of 2D turbulence is simultaneous conservation of energy and enstrophy in the inviscid limit which gives rise to the coexistence of two spectral transfer processes, up-scale for energy and down-scale for enstrophy (see Batchelor[1] and Kraichnan[2]). Gama and Frisch[3] refer to the up-scale, or inverse energy cascade as ''one of the most remarkable phenomenon of two-dimensional turbulence.'' Even though 2D turbulence admits a countable set of integrals of motion (the so-called Casimirs), the integrals of energy and enstrophy provide the dominant conservation laws governing the triad wave number interactions (Vallis[4]) giving rise to such elegant analytical results as, for instance, the Førtoft theorem (Lesieur[5]). These conservation laws are valid in both continuous and discrete Fourier space representations (Vallis[4]). In an infinite domain, the inverse energy cascade precludes the existence of a steady state, since the energy injected into the system with the rate $\overline{\epsilon}$ at some finite wave number mode k_f propagates to ever smaller wave numbers $k<k_f$ with the same rate $\overline{\epsilon}$. However, it is possible to attain a quasi-steady state in the range of the wave numbers that are embedded inside the ''energy front,'' in which case the rate of the energy flux through any Fourier mode k is constant and equal to $\overline{\epsilon}$. Such a quasi-steady state system has been described by the classical Kolmogorov–Batchelor–Kraichnan (KBK) theory (Batchelor,[1] Kraichnan,[2] Mirabel and Monin,[6] Lesieur,[5] Vallis,[4] Frisch[7]) that predicts the energy spectrum

$$E(k)=C_k\overline{\epsilon}^{2/3}k^{-5/3}, \tag{1}$$

where $C_k\cong 6.0$ is the Kolmogorov constant for 2D turbulence. All the basic features of small scale forced 2D turbulence, including the inverse cascade and spectrum in Eq. (1) with $C_k = 6.5 \pm 1$ have been confirmed in recent experiments by Paret and Tabeling.[8]

The inverse cascade and large scale energy saturation in finite systems have prompted the exploration of the analogies between 2D turbulence and Bose gas. Indeed, some of the early statistical theories of 2D turbulence have advanced the conceptual models of a set of large number of the interacting point vortices that form a Hamiltonian system in an inviscid limit. Such vortices were found to be engaged in the energy transfer from small to large scales. More specifically, an analog to the Schrödinger equation was derived for the characteristic functional of the vorticity field that describes a quantum Bose field in a process of coagulation of two bosons into one. Further exploration of this approach allows one to establish the correspondence between quasi-equilibrium 2D turbulence and the ideal Bose gas, and then to draw analogy between turbulence energy saturation at some minimum wave number k_0 and Bose condensation (Mirabel and Monin,[6] Kraichnan[2]). In line with these observations, Borue[9] has advanced the view of the inverse energy cascade as a succession of vortex mergers. However, more detailed analysis indicates that the real picture may be far more complicated; for instance, Dritschel[10] has noted that vortex mergers in 2D turbulence produce not one, but two vortices, one of which is bigger and the other one is smaller than the initial vortices. An excellent modern review of the physics of 2D turbulence and of the application of the methods of statistical mechanics to understand it is given by Frisch.[7]

The validation of the KBK theory in numerical experiments presents a challenge to computational fluid dynamics as invariably only a limited computational domain can be utilized. Then, due to the condensation, energy tends to accumulate in the lowest available wave number modes (Mirabel and Monin,[6] Hossain *et al.*,[11] Kukharkin,[12] Kukharkin *et al.*,[13] Smith and Yakhot[14,15]) leading to unrealistically high velocities and subsequently, numerical instabilities. To prevent such energy condensation, various researchers have used a large scale energy sink parameterized via infrared hyperviscosities of different orders whose action was to suppress the energy of the lowest modes and to ensure reaching the steady state. The energy injected into the system at relatively high wave number modes with the rate $\overline{\epsilon}$ is damped around $k_{\min}$, the minimum explicit wave number of the system, with the same rate $\overline{\epsilon}$, and the modes with $k < k_{\min}$ become essentially irrelevant since they carry very little energy. With few exceptions, simulations with large scale drag reveal the emergence of strong coherent vortices, i.e., vortices that persist for times far exceeding τ_{tu}, the large scale eddy turnover time.

The emergence of coherent vortices in a randomly forced flow field in either energy or enstrophy transfer subrange has been demonstrated both in experimental and computer simulated flows. The laboratory analogs of such vortices were observed, for instance, in experiments with 2D turbulence in a rotating cylindrical tank by Hopfinger *et al.*[16] and in freely decaying 2D turbulence by Tabeling *et al.*[17] In numerical simulations, the emergence and development of coherent vortices were observed and extensively discussed in the pioneering works by Fornberg,[18] Basdevant *et al.*,[19] and McWilliams[20] for the case of freely decaying turbulence. Such vortices were also observed in numerous simulations conducted since then with both unforced, freely decaying 2D turbulence, and forced turbulence in both regimes of enstrophy (for instance, Legras *et al.*[21]) and energy (for instance, Borue[9]) transfer. Thus it is accepted today that 2D turbulent flows in both energy and enstrophy subranges are prone to spontaneous emergence of coherent vortices caused by intrinsic instabilities.

The coherent vortices have been known to affect the statistical properties of the flow field and to hamper the applicability of the statistical mechanics methods to 2D turbulence (Herring and Kerr[22]). Thus in some analyses (Borue,[9] Benzi *et al.*[23,24]), the contribution of coherent vortices to spectral characteristics of the flow was filtered out, rendering the statistics of the remaining structureless background in good agreement with the KBK theory. On the other hand, the detailed analysis of the vorticity structure gave rise to doubts about the applicability of the spectral representation for turbulence description altogether as it does not differentiate between sharply focused coherent vortices and the rest of the chaotic vorticity field (Dritschel[10]).

The mechanism of coherent structures generation and evolution is not well understood and continues to be a subject of the ongoing research (Dritschel[10,25,26]). In addition, such structures are not always present: in simulations by Maltrud and Vallis[27] that employed a piecewise-linear large scale drag, coherent structures were not detected, the energy spectrum preserved the Kolmogorov $-5/3$ distribution for the entire length of integration, and only small, near forcing scale vortices were observed. In a laboratory setting by Paret and Tabeling[8] with strong bottom friction, a linear large scale drag was assumed to be at work, and coherent structures were not observed for the length of the experiment which was about 45 large scale eddy turnover times. However, with increased Reynolds numbers and decreased friction they observed large scale energy saturation and changes in the flow regime. Borue[9] suggested that coherent vortices in the energy subrange of 2D turbulence emerge as the result of anomalous fluctuations and that nearly Gaussian, Kolmogorov-like background $k^{-5/3}$ field is unstable to the formation of such vortices. Insufficient length of integration time and small magnitudes of the ultraviolet and/or infrared Reynolds numbers were singled-out by Borue[9] as the factors that prevented strong deviation from $k^{-5/3}$ scaling in some of the previous simulations. These suggestions were quite general and believed to be independent of particular choice of the infrared hyperviscosity.

On the other hand, Smith and Yakhot[14] questioned the role of the boundaries of the computational domain in the process of coherent vortices formation. They conducted high resolution simulations (2048×2048) with no large scale energy withdrawal at all. The main focus of their paper was the evolution of 2D turbulence before energy saturates at the largest computational scale. It was found that during that short time, the flow field remains structureless and nearly Gaussian while the energy spectrum follows the Kolmogorov scaling Eq. (1) quite closely. Only after the inverse cascade expanded to the smallest available wave number modes where it was blocked from farther unfolding, the condensation had commenced. Then, a system of two large and strong coherent vortices was quickly established; from that point on, the Kolmogorov spectrum was observed no longer. Smith and Yakhot[14,15] thus concluded that, in the energy subrange of 2D turbulence, the generation of coherent vortices, or crystallization, is solely due to the disturbance of the inverse energy cascade brought about by the boundaries of the computational domain.

The inverse cascade can be distorted not only due to finiteness of the computational domain, as in Smith and Yakhot,[14,15] but also due to a choice of the large scale energy withdrawal formulation that is inconsistent with the Kolmogorov dynamics. As will become clear later, indeed, this problem is typical of most of the existing large scale energy dissipation representations.

Based upon the preceding discussion, two possible mechanisms of emergence and development of coherent vortices in the energy subrange can be delineated. First, coherent structures in 2D turbulence result from the intrinsic instability of the nearly Gaussian flow field and are the fundamental feature of the flow dynamics. Alternatively, they are the product of the inverse energy cascade distortion by external factors. The implications of these two mutually exclusive possibilities are rather far reaching since, if the first conjecture were correct, then the KBK steady state would have been irreproducible. As was shown by Smith and Yakhot,[14,15] the second mechanism is at work for nonsteady state turbulence where the inverse cascade causes energy saturation of the lowest resolved modes. For steady state simulations with large scale drag, the situation is not as clear; studies in which the large scale energy withdrawal would be accomplished in such a way as to minimize the distortion of the inverse energy cascade have not been performed.

Here, we present the results of long term, steady state simulations in which the large scale drag emulates the situation where all modes, including the lowest ones, adhere to KBK dynamics, and thus the inverse energy cascade remains undisturbed at all times. Since in finite box simulations $k_{\min}=1$ and there are no smaller wave numbers available, a virtual minimum wave number is introduced, which will be denoted as k_{ls}, $k_{ls}>1$, and the modes with $k<k_{ls}$ are made inactive. Referring to these modes as *supergrid scale* (SPGS) modes and assuming that they all adhere to Kolmogorov spectrum Eq. (1), one can develop an SPGS parameterization which accounts for the energy and enstrophy exchange between those SPGS (or implicit) modes and explicit modes with $k\geqslant k_{ls}$. The derivation of such SPGS representation is analogous to that of the two-parametric viscosity by Kraichnan[28] and is given in the next section. Then, Secs. III and IV describe the application of this new large scale drag parameterization to DNS and LES of 2D turbulence in the energy subrange. One of the central findings of these simulations is the absence of the coherent vortices formation; the flow field remains structureless and Kolmogorovian for practically unlimited integration time. The results and their implications are discussed in the last section.

II. FORMULATION OF THE TWO-PARAMETRIC LARGE SCALE DRAG FOR 2D TURBULENCE

Homogeneous, isotropic, forced, and dissipative 2D turbulence is governed by the vorticity equation

$$\frac{\partial \zeta}{\partial t}+\frac{\partial(\nabla^{-2}\zeta,\zeta)}{\partial(x,y)}=\nu_0\nabla^2\zeta+\xi, \tag{2}$$

where ζ is the fluid vorticity, ν_0 is the molecular viscosity, and ξ is the external forcing. Since the main focus of this paper is the energy cascade subrange, it is assumed that the forcing is localized around some high wave number k_f and is random, zero-mean, Gaussian, and white-noise in time, which is similar to that used by Chekhlov *et al.*[29] To achieve a steady state in numerical simulations based upon Eq. (2), one needs to introduce an additional term in its right hand side, the large scale drag D_{ls}, which provides for the large scale energy dissipation. Usually, D_{ls} is represented by either a Rayleigh (linear or piecewise-linear) drag related to the Ekman boundary layer friction in a geophysical context (McWilliams,[20] Maltrud and Vallis,[27] Pedlosky[30]), or higher order, more scale selective, infrared hyperviscosity (Vallis,[4] Kukharkin,[12] Chekhlov *et al.*[31]).

However, in the inertial range of 2D turbulence, the large scale energy does not dissipate, but cascades to ever lower wave number modes. Therefore, the function of the large scale drag should rather be an *emulation* of the up-scale energy transfer from explicit ($k>k_{ls}$) to supergrid ($k<k_{ls}$) modes while preserving the dynamical processes that would prevail in the case of the infinite domain. The implementation of such large scale drag consists of suppressing the amplitudes of all the modes with $k<k_{ls}$ (SPGS modes) while accounting for their effect on the resolved modes via k-dependent D_{ls} in Eq. (2). In this respect, the physical meaning of the large scale drag is quite similar to that of the two-parametric eddy viscosity (Kraichnan,[28] Chekhlov *et al.*[31]); the difference is in that the latter accounts for the energy exchange between a resolved mode k and all subgrid scale (SGS) modes $k>k_c$ (k_c being the wave number of the dissipation cutoff corresponding to the grid resolution), while the former accounts for the interaction between a resolved mode k and all SPGS modes $k<k_{ls}$. Therefore, similarly to SGS, proper SPGS representation can be derived via introduction of a two-parametric large scale drag, $D(k_{ls}|k)=D_{ls}$, in analogy with the two-parametric viscosity by Kraichnan[28] based upon the evolution equation for the spectral enstrophy density $\Omega(k,t)\equiv(4\pi)^{-1}k\langle\zeta(\mathbf{k},t)\zeta(-\mathbf{k},t)\rangle$, where $\langle ...\rangle$ denotes ensemble averaging:

$$(\partial_t+2\nu_0k^2)\Omega(k,t)=\mathcal{T}_\Omega(k,t). \tag{3}$$

Here, the enstrophy transfer function $\mathcal{T}_\Omega(k,t)$ is given by

$$\mathcal{T}_\Omega(k,t)=\frac{k}{2\pi}\Re\left\{\int_{\mathbf{p}+\mathbf{q}=\mathbf{k}}\frac{\mathbf{p}\times\mathbf{q}}{p^2}\langle\zeta(\mathbf{p},t)\zeta(\mathbf{q},t)\times\zeta(-\mathbf{k},t)\rangle\frac{d\mathbf{p}\,d\mathbf{q}}{(2\pi)^2}\right\}. \tag{4}$$

For a system in statistical steady state the two-parametric transfer $\mathcal{T}_\Omega(k_{ls}|k)$ is calculated from Eq. (4) by extending integration only over all such triangles ($\mathbf{k}$, $\mathbf{p}$, $\mathbf{q}$) that $|k-p|<q<k+p$ and p and/or q are smaller than k_{ls}. Then, the two-parametric large scale drag is defined as

$$D(k_{ls}|k)=-\frac{\mathcal{T}_{\Omega}(k_{ls}|k)}{2k^2\Omega(k)}. \tag{5}$$

In a wide class of quasi-normal approximations $\mathcal{T}_{\Omega}(k_{ls}|k)$ in two dimensions is given by

$$\mathcal{T}_{\Omega}(k_{ls}|k)=\frac{2k}{\pi}\iint_{\Delta}\Theta_{-k,p,q}(p^2-q^2)\sin\alpha\left[\frac{p^2-q^2}{p^3q^3}\Omega(p)\Omega(q)-\frac{k^2-q^2}{k^3q^3}\Omega(q)\Omega(k)+\frac{k^2-p^2}{k^3p^3}\Omega(p)\Omega(k)\right]dp\,dq, \tag{6}$$

where $\Theta_{-k,p,q}$ is the triad relaxation time. Also, the angle α is formed by the vectors $\mathbf{p}$ and $\mathbf{q}$, and $\iint_{\Delta}$ denotes integration over the area defined above.

Different spectral closure models provide different expressions for $\Theta_{-k,p,q}$. Here, $\Theta_{-k,p,q}$ was calculated using the renormalization group theory of turbulence (Staroselsky and Sukoriansky,[32] Sukoriansky *et al.*[33]). Numerical integration of Eq. (6), using the assumption that all the SPGS modes $k<k_{ls}$ adhere to Kolmogorov spectrum Eq. (1), yields the large scale drag representation

$$D(k_{ls}|k)=0.0974\bar{\epsilon}^{1/3}k_{ls}^{-4/3}F(k/k_{ls}), \tag{7}$$

where $F(x)$ is a nondimensional function; $F(1)=1$. The function $F(x)$ is presented in Fig. 1(a), and in log–log format, in Fig. 1(b). One can see that $F(x)$ is not a power law function; for small k (the cusp region) its distribution is close to x^{-2} but for larger x it becomes steeper. The least square approximation gives $F(x)\approx x^{-2.58}$ for $x\geqslant 1$.

In a large number of simulations reported in the literature, the large scale drag has been represented by the infrared hyperviscosity,

$$F(x)\sim x^{-2n}, \quad n\geqslant 1, \tag{8}$$

while the coefficient was set based upon Reynolds number similarity considerations. Comparing Eq. (8) to Fig. 1(b) one should note important differences: first, the approximation Eq. (8) is inaccurate for $x>1$ which can be expected to distort the energy exchange among the explicit modes as well as between the explicit and SPGS modes resulting in disturbing the inverse energy cascade and, second, Eq. (8) is singular for $x\rightarrow 0$, while in the present large scale drag parameterization, $F(x)$ is undefined for $x<1$.

To implement the two-parametric large scale drag parameterization in spectral DNS of 2D turbulence, one needs to replace Eq. (2) by equation for the resolved Fourier modes that includes Eq. (5) in its right hand side,

$$\frac{\partial\zeta(\mathbf{k})}{\partial t}+\int_{|p|,|k-p|>k_{ls}}\frac{\mathbf{p}\times\mathbf{k}}{p^2}\zeta(\mathbf{p})\zeta(\mathbf{k}-\mathbf{p})\frac{d\mathbf{p}}{(2\pi)^2}=-\nu_0k^2\zeta(\mathbf{k})-D(k_{ls}|k)k^2\zeta(\mathbf{k})+\xi(\mathbf{k}), \quad k\geqslant k_{ls}>1. \tag{9}$$

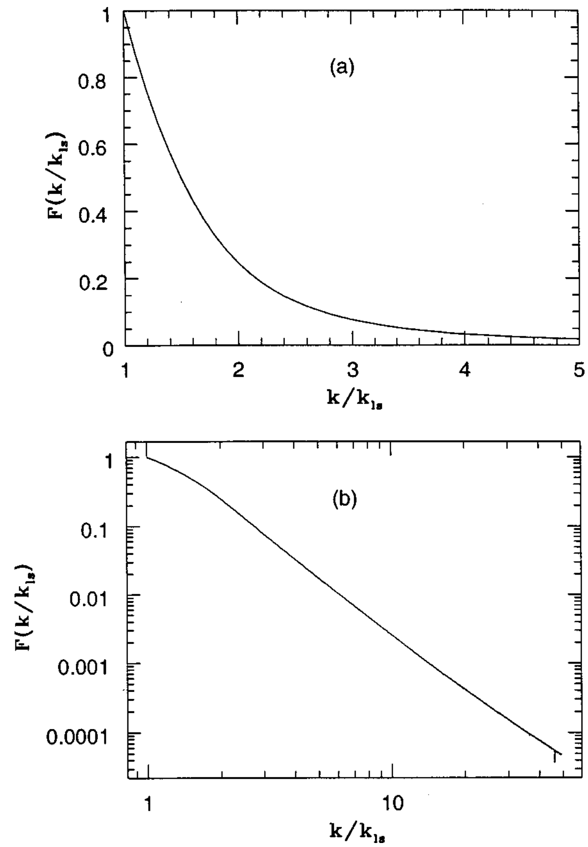

FIG. 1. Nondimensional function $F(x)$ used in the new large scale drag representation Eq. (7) in linear–linear (a) and log–log (b) scalings.

The viscous term in Eq. (9) is routinely replaced by a higher order hyperviscous term (Borue,[9] McWilliams,[20] Maltrud and Vallis,[27] Chekhlov *et al.*[31]). If k_{ls} is set at too small a value (1 or 2), then one needs to resort to discrete spectrum based derivation of $D(k_{ls}|k)$ using Eq. (6), which will be inconsistent with the present calculation based upon the continuous spectrum. Therefore, to allow for sufficient number of discrete modes to be involved in derivation of $D(k_{ls}|k)$, k_{ls} should be set sufficiently large. Upon specifying the value of k_{ls}, the amplitudes of the modes with $1\leqslant k<k_{ls}$ are set to zero at every time step (''chopping'').

The large scale drag parameterization based upon Eq. (7) can be used in LES, in which case Eq. (9) should be replaced by equation for the explicit Fourier modes that in addition to SPGS also includes SGS representation,

$$\frac{\partial\zeta(\mathbf{k})}{\partial t}+\int_{k_{ls}<|p|,|k-p|<k_c}\frac{\mathbf{p}\times\mathbf{k}}{p^2}\zeta(\mathbf{p})\zeta(\mathbf{k}-\mathbf{p})\frac{d\mathbf{p}}{(2\pi)^2}=-\nu(k|k_c)k^2\zeta(\mathbf{k})-D(k_{ls}|k)k^2\zeta(\mathbf{k}), \quad k\in[k_{ls},k_c], \tag{10}$$

where $\nu(k|k_c)$ is the two-parametric viscosity; its implementation in 2D LES will be described in Sec. IV. It is important to emphasize that the new large scale drag representation, be it used either in DNS or LES, combines both Eq. (7) and chopping.

The new SPGS parameterization Eq. (7) is designed to preserve the KBK flow regime for as long as it remains stable. Eliminating the boundary effects from the list of potential instability sources, the new large scale drag formulation enables us to conduct long term studies of the initially KBK flow regime and to determine its stability.

As a side remark, let us note that Eq. (10) admits yet another interpretation. The fact that the range of the resolved modes is confined from both sides, i.e., by k_{ls} and k_c, means that only *intermediate* scales are explicitly resolved. Thus the computational model given by Eq. (10) should be, strictly speaking, referred to as ''mid eddy simulation.'' This tool may be quite useful in simulations of turbulent flows, and Eq. (10) provides a framework representing the effects of the implicit modes upon the explicit ones in such simulations. Throughout this paper, however, a more traditional term ''LES'' will be used.

In the following two sections featuring DNS and LES of 2D turbulence in the energy subrange, it will be shown that the new SPGS representation allows for establishing a steady state, stable, structureless flow regime that adheres to KBK statistical laws for the entire length of integration.

III. DNS OF 2D TURBULENCE WITH TWO-PARAMETRIC LARGE SCALE DRAG

To study the effect of the large scale drag formulation on evolution of 2D turbulence in the energy transfer subrange, three different DNS were arranged for. The first DNS (DNS1) was conducted with no large scale drag at all, while in the second DNS (DNS2), an algebraic formulation Eq. (8) with $n=6$ was used. Finally, in the third DNS (DNS3), the new two-parametric formulation Eq. (7) was employed. The chopping for $k<k_{ls}=8$ was introduced in both DNS1 and DNS3, while in DNS2, the algebraic large scale drag was essentially suppressing the modes in the same range. Thus the only difference between the various DNS was their large scale drag formulation.

The setting of all present numerical experiments was very similar to our previous simulations described in Chekhlov *et al.*[31,29] The most significant difference was the increase in resolution from 512^2 to 1024^2 Fourier modes. Very briefly, the present DNS were based on a fully dealiased pseudospectral Fourier method to solve Eq. (9) in a periodic box x, $y\in[0,2\pi]\times[0,2\pi]$ with doubly periodic boundary and zero initial conditions. The dealiasing was based upon the 2/3 rule. The time discretization was the same as in Chekhlov *et al.*[31] The forcing ξ was given by $\xi(k,t) = A_\xi \sigma_k(t)/\sqrt{\delta t}$ for $k\in[215,222]$ and zero otherwise; here, $\delta t=1$ is the time step, and $\sigma_k(t)$ is a discrete and uncorrelated in time, Gaussian random number with unit variance. To extend the inertial subrange, a high order, small scale, hyperviscous term $A_s k^{14}$ was added to the right hand side of Eq. (9) replacing the viscous term. The coefficient $A_s(=2.9\times10^{-41})$ was set in the range where it almost does not affect the forcing scale but ensures effective dissipation of the modes with $k>k_f$.

Figures 2(a)–(c) show the time history of the total energy for all three DNS performed. The energy here is normalized by E_K, the total energy obtained by integrating the Kolmogorov spectrum Eq. (1) between $k_{ls}=8$ and $k_f=215$.

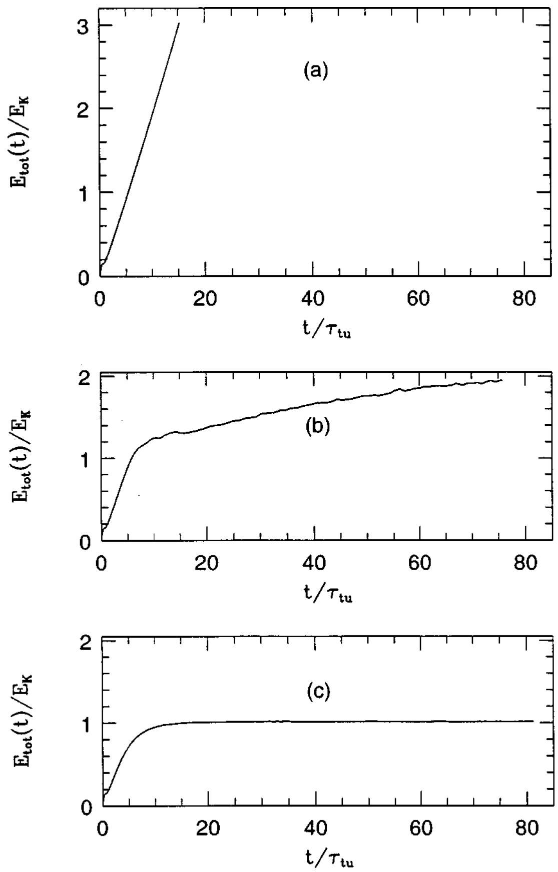

FIG. 2. Evolution of the total energy normalized by the corresponding Kolmogorov value for DNS1 (a), DNS2 (b), and DNS3 (c).

One can see that in both DNS1 and DNS2, the energy was steadily growing in time exceeding E_K already after about $5\tau_{tu}$. Not only the steady state was unreachable in these DNS, but growing velocities eventually lead to violation of the Courant criterion and development of numerical instability. The onset of instability can be delayed somewhat by gradual decrease of the time step; the procedure used by Smith and Yakhot[15] in simulations similar to DNS1 here. In this case, however, the instability can be expected to be preceded by crystallization or formation of the regular lattice of vortices, as observed in Ref. 15. On the contrary, in DNS3, the total energy equilibrated at the level of E_K after about $10\tau_{tu}$ and remained constant and approximately equal to E_K for the rest of the integration. Here, due to the limited computer resources, the integration was extended to about $80\tau_{tu}$. However, the robustness of the steady state achieved indicates that the integration could be continued for a considerably longer time.

Figures 3(a)–(c) show the evolution of the total enstrophy for all three DNS. This enstrophy is normalized by Ω_K, the total enstrophy obtained by integrating the Kolmogorov spectrum Eq. (1) in the same range as for the total energy. One can see that unlike the total energy, the total enstrophy, after the initial overshoot, equilibrates reasonably quickly in all three DNS and stays at the level of about $1.5\Omega_K$. The factor of 1.5 can be understood recalling that a major contribution into the total enstrophy integral comes from the high

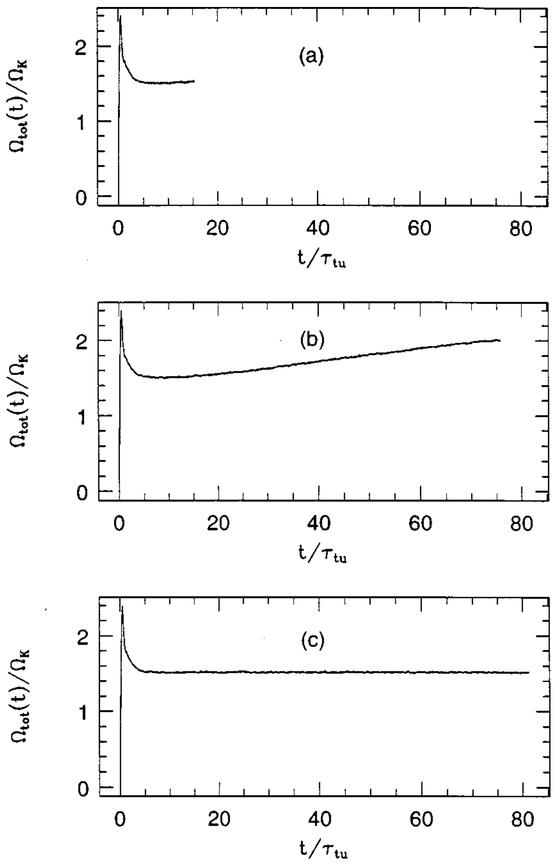

FIG. 3. Evolution of the total enstrophy normalized by the corresponding Kolmogorov value for DNS1 (a), DNS2 (b), and DNS3 (c).

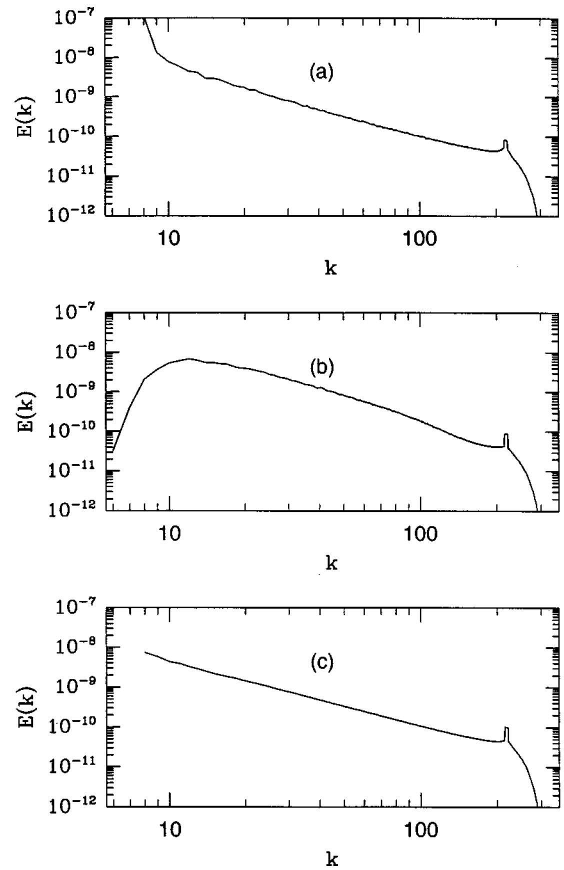

FIG. 4. Averaged energy spectrum sampled close to the end of integration; (a) DNS1, (b) DNS2, (c) DNS3.

wave number modes, which are the forcing modes k_f and the modes adjacent to them. The near steady state in total enstrophy can be understood if one recalls that in the present simulations, there exists a direct enstrophy cascade but at the high wave numbers, enstrophy is effectively dissipated by the high power law hyperviscosity. The total enstrophy remains constant in DNS3 but is growing slowly in DNS2 due to the low mode energy condensation.

Figures 4(a)–(c) depict the averaged spectra for all DNS sampled close to the end of integration. In DNS1 and DNS2, one can clearly see that the spectrum begins to deviate from the Kolmogorov law Eq. (1) at the lower wave number end which is the direct result of the energy accumulation in large scale coherent structures. In DNS3, however, the spectrum remains almost perfectly Kolmogorov-like for the entire length of integration, which is achieved here solely due to the proper choice of SPGS parameterization Eq. (7).

Figures 5(a)–(c) show the compensated energy spectrum, $E(k)\overline{\epsilon}^{-2/3}k^{5/3}$, for all three DNS. One can see that in DNS1 and DNS2, due to strong deviations from the Kolmogorov regime, the compensated energy spectrum is k-dependent. Since the spectrum was evolving in time, the available averaging time was short. On the other hand, in DNS3, the compensated spectrum is in a robust steady state, is nearly k-independent and is very close to the Kolmogorov constant which is known to be about 6. Thus Fig. 5(c) provides one more evidence that, with the new large scale drag parameterization, a 2D turbulent flow field attains a robust steady state with nearly Kolmogorov dynamics.

Figure 6 presents the evolution of the compensated energy spectrum for DNS2. One can clearly see that this spectrum is not only k-dependent at all times but also is time dependent gradually attaining ever increasing values as a result of the progressive large scale energy condensation.

An insightful characteristic of the energy transfer processes through a wave number k in 2D turbulence is the total energy flux $\Pi(k)$ from all the modes $\in(k,\infty)$ to all the modes $\in(0,k)$. Since in our simulations the modes with $k < k_{ls}$ are not allowed, their effect is emulated by the large scale drag Eq. (7). Theoretically, one expects that $\Pi(k)/\overline{\epsilon} = 1$ for all k. Figures 7(a)–(c) show the ratio $\Pi(k)/\overline{\epsilon}$ obtained in all three DNS. Figures 7(a)(b) indicate that due to the absence of the large scale drag, as in DNS1, or inadequate large scale drag representation by the infrared hyperviscosity, as in DNS2, this ratio deviates from 1, particularly for $k<10$. Only the proposed SPGS parameterization Eq. (7) produces $\Pi(k)/\overline{\epsilon}=1$ for all k, which is yet another indication that the new large scale drag formulation does not distort the intermodal energy exchange.

Finally, Figs. 8(a) and (b) show the color coded maps of the velocity magnitudes for DNS2 and DNS3. One can clearly see that in DNS2, coherent vortices are in the process of organization and growth; in fact, velocity variations may reach an order of magnitude over small distances. On the

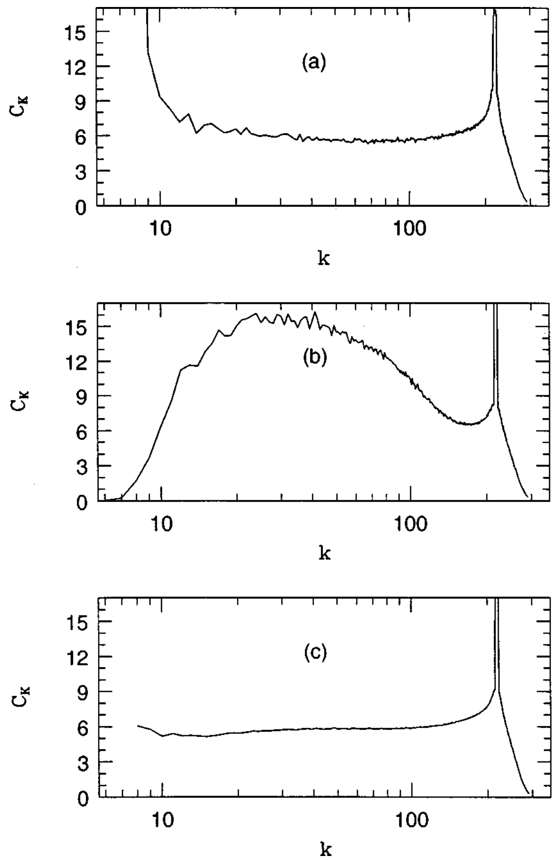

FIG. 5. Same as in Fig. 4 but for compensated energy spectrum.

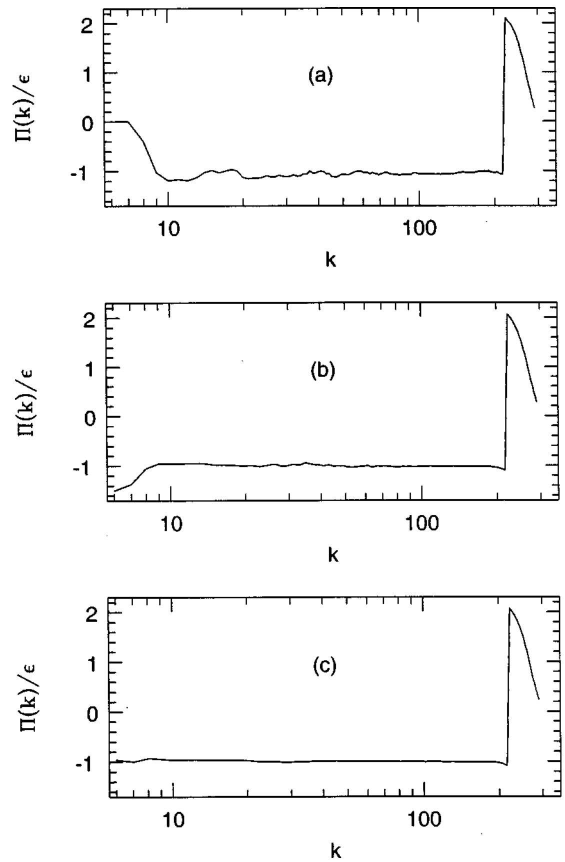

FIG. 7. Total energy transfer function $\Pi(k)$ normalized by the constant energy injection rate $\bar{\epsilon}$ for DNS1 (a), DNS2 (b), and DNS3 (c), respectively.

contrary, in DNS3 the flow field appears structureless with total velocity changes not exceeding the factor of 2 or 3. Note that if the infrared hyperviscosity is used, the development of strong coherent vortices requires a very long integration time—Borue,[9] for instance, continued his simulations for about $300\tau_{tu}$. The reason for such a long time obviously is the suppression of the energy of the lowest modes. With the resolution of 1024^2 Fourier modes, such a long integration was computationally prohibitive in the present study and was not attempted. Bearing in mind that generation of coherent vortices in simulations similar to DNS1 and DNS2 has been well observed and established (for instance, Borue,[9] Smith and Yakhot[15]), we show Figs. 8(a), (b) to merely illustrate that the difference in the flow structure in physical space is consistent with the spectral characteristics shown in Figs. 2(a)–(c) and 4(a)–(c). More specifically, growing in time total energy [Figs. 2(a), (b)] and steepening of the low wave number end of the spectra [Figs. 4(a), (b)] are associated with the gradual energy accumulation in coherent vortices clearly visible in Fig. 8(a). On the other hand, with the new large scale drag formulation used in DNS3, the total energy spectrum remains nearly Kolmogorovian for the entire length of integration, while in the physical space, the flow field preserves its structureless configuration.

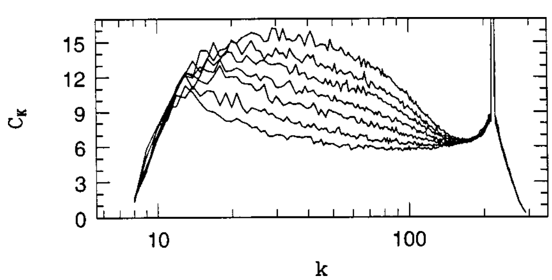

FIG. 6. Evolution of the compensated energy spectrum for DNS2; the time interval between the contours is $10\tau_{tu}$.

Summarizing the information presented in Figs. 2–8, one concludes that the new large scale drag representation allows one to attain a steady state solution in direct numerical simulations of forced, isotropic, homogeneous 2D turbulence in the energy subrange. The flow field in this steady state is structureless and its statistics are in very good agreement with the KBK theory.

IV. LES OF 2D TURBULENCE WITH TWO-PARAMETRIC LARGE SCALE DRAG

The simultaneous conservation of energy and enstrophy in 2D turbulence makes large eddy simulation in the energy subrange with unresolved small scale energy source distinctively different from LES of three-dimensional flows. The major difference occurs in SGS representation of 2D flows. As explained in Sukoriansky *et al.*,[33] it turns out that the presence of the two integrals of motion commands a two-term SGS representation derived from the two-parametric viscosity $\nu(k|k_c)$,

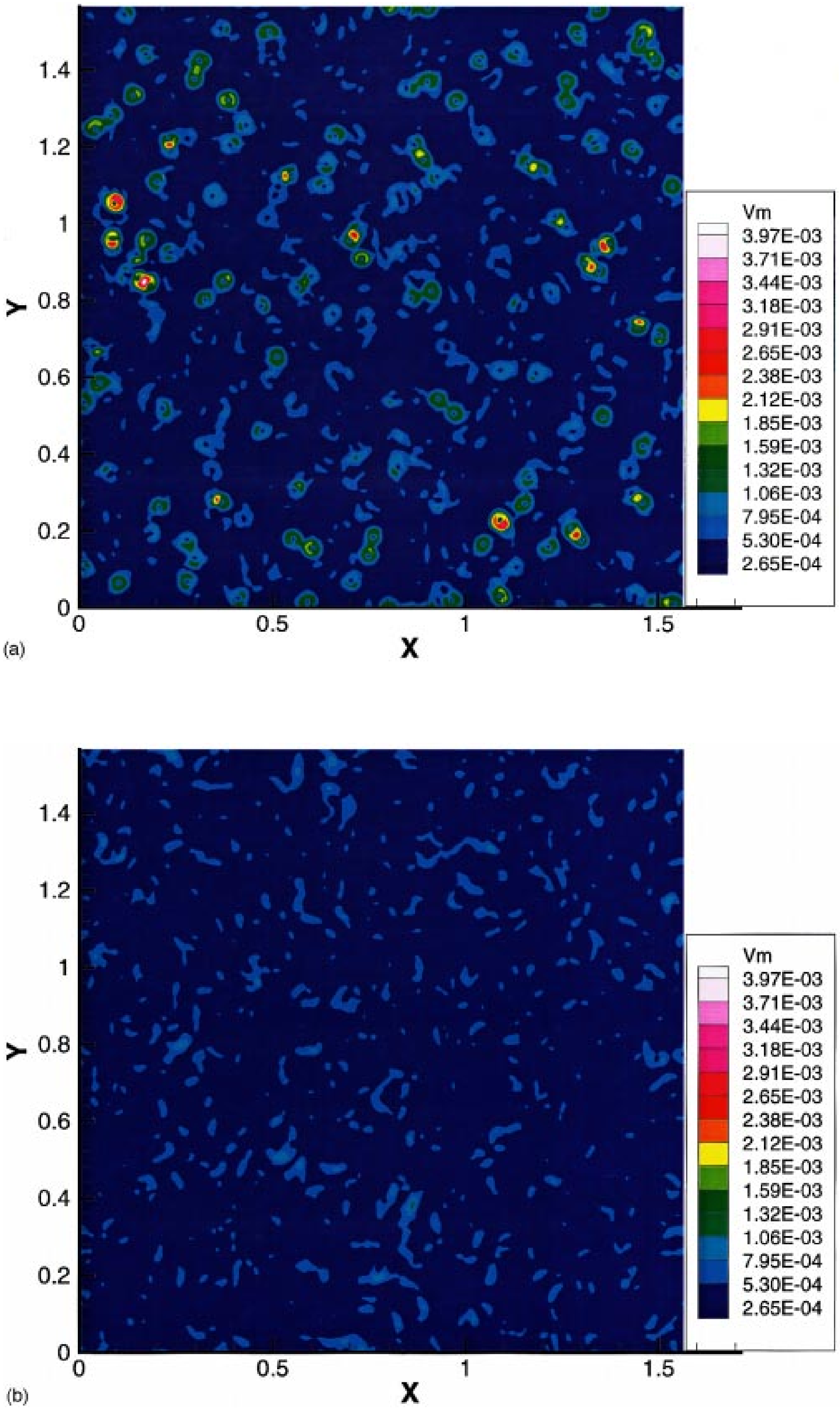

FIG. 8. Color maps of the velocity magnitude in the physical space; (a) DNS2, (b) DNS3.

$$\nu(k|k_c) = -\frac{\overline{\epsilon}}{0.8\overline{\Omega}(t)} + \frac{\overline{\epsilon}}{0.8\overline{\Omega}(t)}\phi(k/k_c), \tag{11}$$

where $\overline{\Omega}(t)$ is the total enstrophy and $\phi(x)>0$ for $0 \leq x \leq 1$. It is essential that Eq. (11) consists of a negative and a positive terms, otherwise the simultaneous conservation of energy and enstrophy cannot be achieved. The first term in Eq. (11) represents the *negative* Laplacian viscosity which accounts for the unresolved small scale forcing, while the second provides the stabilizing dissipation. At first sight, it may look paradoxical that the negative viscosity, which is supposed to provide an energy forcing with a constant rate $\overline{\epsilon}$

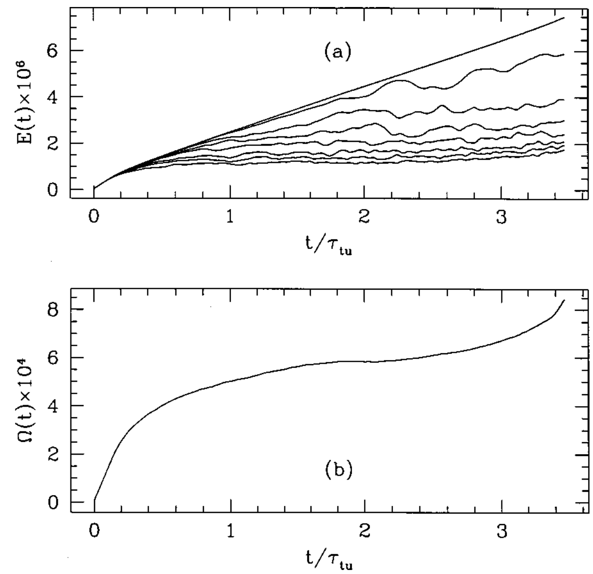

FIG. 9. Evolution of the total energy (a) and enstrophy (b) in LES1. (a) also shows the total energy with the energy of the first, second, third, fourth, fifth, sixth, and seventh modes removed.

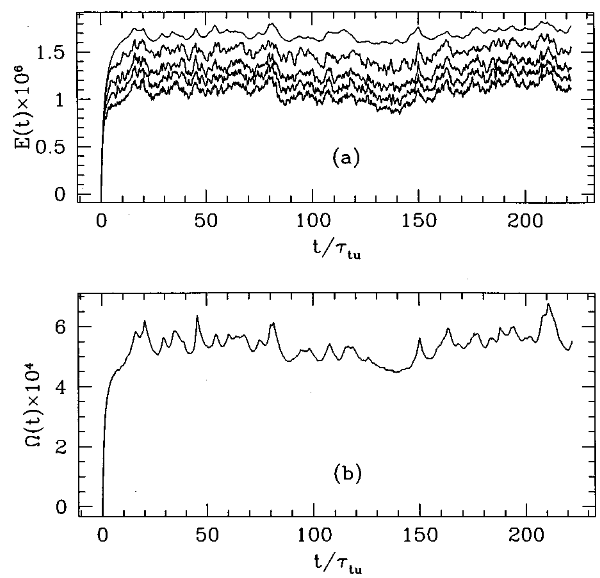

FIG. 10. Same as in Fig. 9 but for LES2.

in Eq. (11), is in fact flow dependent, due to the presence of $\overline{\Omega}(t)$ in its denominator. However, Sukoriansky *et al.*[33] have shown that this flow dependence is crucial for stability of LES; a flow independent negative viscosity would lead to nonlinear growth in time of both total energy and enstrophy due to the positive feedback between energy input and enstrophy of the resolved modes. Sukoriansky *et al.*[33] have also shown that $\phi(k/k_c)$ can be represented by a series in powers of $(k/k_c)^2$ which are equivalent to the hyperviscous dissipation terms in the physical space. The simplest approximation to $\phi(k/k_c)$ is given by $1.6(k/k_c)^2$, where the coefficient 1.6 ensures zero enstrophy transfer in the energy subrange. Although the dissipative terms are essential to the physics and numerical stability of LES, they are much less sensitive to the details of the flow than the negative term; Sukoriansky *et al.*[33] have also shown that flow independent hyperviscosities can ensure robust LES for many tens of large scale turnover times.

The SGS representation that consists of the negative, flow dependent (eddy) viscosity term and positive stabilizing hyperviscous terms has been referred to by Sukoriansky *et al.*[33] as a stabilized negative viscosity (SNV) formulation.

Note that since the SNV scheme includes a negative Laplacian viscosity and a positive biharmonic hyperviscosity, it structurally resembles the Kuramoto–Sivashinsky equation widely known from the combustion theory (Sivashinsky[34]) and flows with chemical reactions (Kuramoto and Tsuzuki,[35] Kuramoto[36]). Papers by Dubrulle and Frisch,[37] Gama and Frisch,[3] and Gama *et al.*[38,39] describe derivation of a negative, flow independent eddy viscosity using the concept of the parity-invariant flow and its utilization in 2D simulations on the Connection machine for marginally negative viscosity situations. Since the equation solved possessed the Navier–Stokes type nonlinearity and Kuramoto–Sivashinsky type large scale instability, the resulting equation was dubbed the Navier–Stokes–Kuramoto–Sivashinsky (NSKS) equation by Gama *et al.*[38] Simulations revealed a period of the linear growth which was then replaced by a disorganized inverse cascade that evolved into a structured vortical regime with proliferating monopolar and multipolar structures with strongly depleted nonlinearities (Gama and Frisch[3]). On the other hand, Kolmogorov type turbulence with the robust inverse cascade, $-5/3$ energy spectrum and structureless flow field, similar to DNS3 described in the previous section, was not observed in these simulations.

The main difference between our SNV formulation and the NSKS equation is in the derivation of SNV and in the flow dependency of its coefficients. In addition, the NSKS equation does not include a large scale drag while an SPGS representation is a very important component of the SNV based LES scheme. One expects that the results of DNS and LES of similar flows should agree. For the NSKS equation,

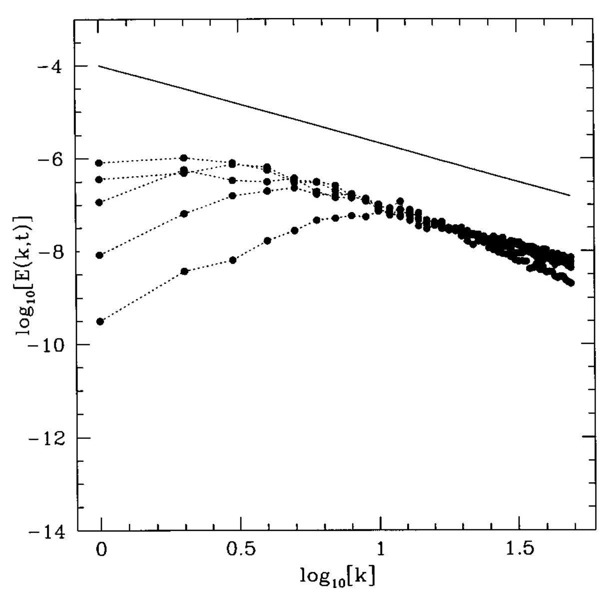

FIG. 11. Evolution of the instantaneous energy spectrum for LES1 for $t/\tau_{tu}=0.56$, 1.11, 1.67, 2.78, and 3.33. The solid line represents Kolmogorov $-5/3$ slope.

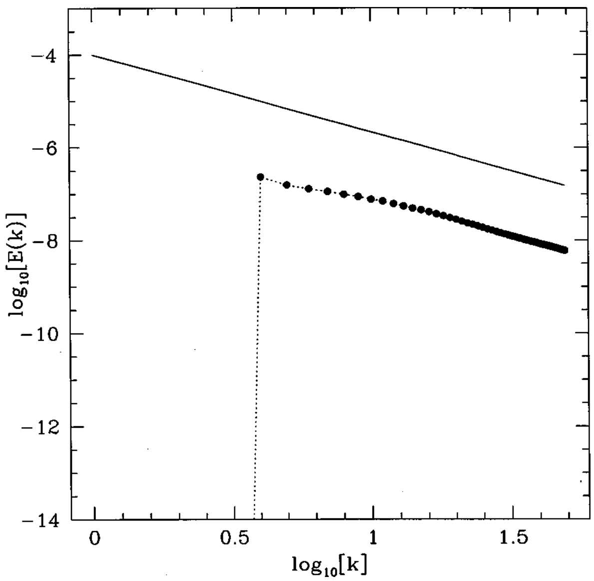

FIG. 12. Time averaged spectrum for LES2.

such comparisons have not been performed; furthermore, the corresponding DNS for that case does not exist. On the other hand, DNS described in the previous section can be used for direct comparisons with the results of SNV based LES with the SPGS parameterization given by Eq. (7). Here, the results of two such LES are described. In these LES, a new SPGS parameterization Eq. (7) was implemented using the LES framework Eq. (10) with the SNV SGS representation Eq. (11). In the main focus of these LES were the existence and statistical properties of a steady state solution to Eq. (10).

The setting of LES was quite similar to DNS described in the previous section. The resolution used was 162^2 Fourier modes with the 2/3 dealiasing rule; the SGS cutoff wave number was set at $k_c=50$. The flow was initialized as zero field everywhere except for a narrow band of wave numbers in the middle part of the spectrum, where it was set random and Gaussian. The energy injection rate was about $\overline{\epsilon}=5.19\times10^{-10}$, the time step was set at $\delta t=0.5$. In LES1, no large scale drag was used, while in LES2, full SGS-SPGS formulation Eqs. (10), (11) was employed with the function $\phi(k/k_c)$ calculated using the renormalization group theory of turbulence, as explained by Sukoriansky *et al.*[33] In addition, in formulation of the large scale drag in LES2 it was set $k_{ls}=4$.

Figures 9 and 10 show the evolution of the total energy and enstrophy in LES1 and LES2. Similarly to DNS1, in LES1 with no large scale drag used, the energy grows linearly in time, Fig. 9(a). Eventually, after inverse cascade expands to the boundaries of the computational domain, LES1 develops instability, while in LES2, with the new SPGS formulation implemented, the total energy equilibrates and remains in near steady state for over $220\tau_{tu}$ as shown in Fig. 10(a).

Figure 9(b) shows that in LES1, the total enstrophy stays equilibrated for up to about $3\tau_{tu}$, until the lowest available wave number modes are reached by the inverse energy cascade, after which $\overline{\Omega}(t)$ grows very rapidly. On the other hand, in LES2, Fig. 9(b), the total enstrophy remains nearly constant for about $220\tau_{tu}$.

Figures 11 and 12 compare the spectra obtained in both LES. In LES1, Fig. 11, the instantaneous spectrum $E(k)$ quickly approaches the Kolmogorov distribution Eq. (1) and preserves it for up to about $t\approx3\tau_{tu}$. For a longer time, the spectrum rapidly deviates from the Kolmogorov scaling until the flow becomes unstable. On the other hand, in LES2, Fig. 12, the spectrum preserves Kolmogorov-like shape practically indefinitely. As mentioned earlier, Kolmogorov turbulence has not been observed in simulations with NSKS equation.

In the physical space, the flow pattern obtained in LES2 is quite similar to that of DNS3—it remains practically structureless and consistent with the Kolmogorov statistics after many turnover times.

Concluding, let us re-emphasize that the results of LES described in this section are consistent with the results of DNS in the previous section. They demonstrate that the new SPGS representation makes it possible to maintain Kolmogorov-like, structureless, steady state flow regime in large eddy simulation of forced, dissipative 2D turbulence for a very long integration time.

V. DISCUSSION AND CONCLUSIONS

The results of DNS and LES presented here indicate that the formulation of the large scale drag is critical in simulations of 2D turbulence in a doubly periodic box, because it is ultimately responsible for the existence and physical nature of the steady state. The widely used in modern simulations infrared hyperviscosities prevent the explosive instability due to the energy saturation of the lowest modes. However, they disturb the inverse energy cascade causing deviations from, and eventual break down of the KBK statistical laws. On the other hand, the proposed here new large scale drag parameterization preserves the steady state, the KBK flow regime for very long integration times thus proving its stability and reproducibility. The presented simulations clearly demonstrate that the emergence of coherent structures is the direct result of the inverse cascade distortion rather than the product of the intrinsic instability.

This study reveals the physically correct way to simulate forced, dissipative, homogeneous and isotropic 2D turbulence in the periodic box setting. Realizing that the large scale drag has a complicated and subtle function in such simulations, a notion of supergrid scales was introduced, and the drag, or SPGS parameterization was defined as a measure of the energy and enstrophy exchange between explicit and SPGS modes. Proper SPGS representation is given by the two-parametric large scale drag which is the SPGS analog of the two-parametric viscosity by Kraichnan.[28]

The simulations presented here describe a highly idealized situation pertaining to homogeneous isotropic 2D turbulence, which is a useful tool to analyze the emergence of coherent structures and stability of KBK regime, the subjects of great theoretical importance. In particular, the results confirmed Smith and Yakhot[15] conjecture that the coherent vortices in small scale forced, quasi-2D turbulent flows are caused by the large scale energy saturation due to finiteness of the domain. In addition, it was shown that the evolving flow regime critically depends on SPGS parameterization. In the reality, flow domains are naturally truncated, and coherent structures are rather common. The present results are indicative of the importance of using a proper SPGS representation in simulations of realistic quasi-2D flows with inverse energy cascade, including nonsteady flows with slowly varying large scale statistics. Even when the physical mechanisms responsible for the large scale energy withdrawal are known, accurate numerical simulations should employ the value of the drag as ''seen'' by the resolved modes. Such a drag would lead to the notion of the ''eddy'' large scale drag, generally expected to be k-dependent. Here, the proper derivation of such an SPGS representation is given provided that the statistical behavior of the largest scales is known. When calculations are concerned with the intermediate scales only, this approach results in a new computational technique, ''mid-eddy simulation.'' This new method may also be useful in nested grid simulations or in problems involving regional modeling in meteorology and physical oceanography. Among important issues that yet need to be addressed in the future research are the derivation of the proper SPGS representation in the physical space and the formulation of the appropriate open boundary conditions for physical space simulations in a limited domain.

ACKNOWLEDGMENTS

The authors would like to thank the anonymous reviewers whose critical and constructive comments helped us to clarify and improve the manuscript. This research has been partially supported by ONR, NSF, NASA, and the Perlstone Center for Aeronautical Engineering Studies. The computations were performed on Cray Y-MP of NAVOCEANO Supercomputer Center, Stennis Space Center, Mississippi, and Cray-J90 of HPCU, Interuniversity Computational Center, Israel.

[1]G. K. Batchelor, ''Computation of the energy spectrum in two-dimensional turbulence,'' Phys. Fluids **12**, 233 (1967).

[2]R. H. Kraichnan, ''Inertial ranges in two-dimensional turbulence,'' Phys. Fluids **10**, 1417 (1967).

[3]S. Gama and U. Frisch, ''Simulations of two-dimensional turbulence on the Connection machine,'' *Advances in Turbulence IV*, edited by F. T. M. Nieuwstadt, Appl. Sci. Res. **51**, 105 (1993).

[4]G. K. Vallis, ''Problems and phenomenology in two-dimensional turbulence,'' in *Nonlinear Phenomena in Atmospheric and Oceanic Sciences*, edited by G. K. Carnevale and R. T. Pierrehumbert (Springer-Verlag, New York, 1992), pp. 1–25.

[5]M. Lesieur, *Turbulence in Fluids*, 2nd ed. (Kluwer, New York, 1990).

[6]A. Mirabel and A. Monin, ''Two-dimensional turbulence,'' Uspechi Mechaniki **2**, 47 (1979) (in Russian).

[7]U. Frisch, *Turbulence* (Cambridge University Press, Cambridge, 1993).

[8]J. Paret and P. Tabeling, ''Experimental observation of the two-dimensional inverse energy cascade,'' Phys. Rev. Lett. **79**, 4162 (1997).

[9]V. Borue, ''Inverse energy cascade in stationary two-dimensional homogeneous turbulence,'' Phys. Rev. Lett. **72**, 1475 (1994).

[10]D. G. Dritschel, ''Vortex properties of two-dimensional turbulence,'' Phys. Fluids A **5**, 984 (1993).

[11]M. Hossain, W. H. Matthaeus, and D. Montgomery, ''Long-time states of inverse cascades in the presence of a maximum length scale,'' J. Plasma Phys. **30**, 479 (1983).

[12]N. N. Kukharkin, ''Coherent structure formation, phase correlations, and finite-size effects in 2D turbulence,'' J. Sci. Comput. **10**, 409 (1995).

[13]N. Kukharkin, S. A. Orszag, and V. Yakhot, ''Quasicrystallization of vortices in drift-wave turbulence,'' Phys. Rev. Lett. **75**, 2486 (1995).

[14]L. M. Smith and V. Yakhot, ''Bose condensation and small-scale structure generation in a random force driven 2D turbulence,'' Phys. Rev. Lett. **71**, 352 (1993).

[15]L. M. Smith and V. Yakhot, ''Finite-size effects in forced two dimensional turbulence,'' J. Fluid Mech. **274**, 115 (1994).

[16]E. Hopfinger, F. Browand, and Y. Gagne, ''Turbulence and waves in a rotating tank,'' J. Fluid Mech. **125**, 505 (1982).

[17]P. Tabeling, S. Bukhart, O. Cardoso, and H. Willaime, ''Experimental study of freely decaying two-dimensional turbulence,'' Phys. Rev. Lett. **67**, 3772 (1991).

[18]B. Fornberg, ''A numerical study of 2D turbulence,'' J. Comput. Phys. **25**, 1 (1977).

[19]C. Basdevant, B. Legras, B. Sadourny, and M. Béland, ''A study of barotropic model flows: intermittency, waves and predictability,'' J. Atmos. Sci. **38**, 2305 (1981).

[20]J. C. McWilliams, ''The emergence of isolated coherent vortices in turbulent flow,'' J. Fluid Mech. **146**, 21 (1984).

[21]B. Legras, P. Santangelo, and R. Benzi, ''High-resolution numerical experiments for forced two-dimensional turbulence,'' Europhys. Lett. **5**, 37 (1988).

[22]J. R. Herring and R. M. Kerr, ''Some contributions of two-point closure to large eddy simulation,'' in *Large Eddy Simulation of Complex Engineering and Geophysical Flows*, edited by B. Galperin and S. A. Orszag (Cambridge University Press, Cambridge, 1993), pp. 79–104.

[23]R. Benzi, R. Patarnello, and P. Santangelo, ''On the statistical properties of two-dimensional decaying turbulence,'' Europhys. Lett. **3**, 811 (1987).

[24]R. Benzi, R. Patarnello, and P. Santangelo, ''Self-similar coherent structures in two-dimensional decaying turbulence,'' J. Phys. A: Math. Gen. **21**, 1221 (1988).

[25]D. G. Dritschel, ''A general theory for two-dimensional vortex interactions,'' J. Fluid Mech. **293**, 269 (1995).

[26]D. G. Dritschel, ''On the persistence of nonaxisymmetric vortices in inviscid two-dimensional flows,'' J. Fluid Mech. **371**, 141 (1998).

[27]M. E. Maltrud and G. K. Vallis, ''Energy spectra and coherent structures in forced two-dimensional and beta-plane turbulence,'' J. Fluid Mech. **228**, 321 (1991).

[28]R. H. Kraichnan, ''Eddy viscosity in two and three dimensions,'' J. Atmos. Sci. **33**, 1521 (1976).

[29]A. Chekhlov, S. A. Orszag, S. Sukoriansky, B. Galperin, and I. Staroselsky, ''The effect of small-scale forcing on large-scale structures in two-dimensional flows,'' Physica D **6**, 2548 (1996).

[30]J. Pedlosky, *Geophysical Fluid Dynamics*, 2nd ed. (Springer-Verlag, New York, 1987).

[31]A. Chekhlov, S. A. Orszag, S. Sukoriansky, B. Galperin, and I. Staroselsky, ''Direct numerical simulation tests of eddy viscosity in two dimensions,'' Phys. Fluids **6**, 2548 (1994).

[32]I. Staroselsky and S. Sukoriansky, ''Renormalization group approach to two-dimensional turbulence and the ϵ-expansion for the vorticity equation,'' in *Advances in Turbulence Studies*, edited by H. Branover and Y. Unger, Progress in Astron. and Aeron. (American Institute of Aeronautics and Astronautics, Inc., Washington, DC, 1993), Vol. 149, pp. 159–164.

[33]S. Sukoriansky, A. Chekhlov, S. A. Orszag, B. Galperin, and I. Staroselsky, ''Large eddy simulation of two-dimensional isotropic turbulence,'' J. Sci. Comput. **11**, 13 (1996).

[34]G. I. Sivashinsky, ''Nonlinear analysis of hydrodynamic instability in laminar flames-I. Derivation of basic equations,'' Acta Astron. **4**, 1177 (1977).

[35]Y. Kuramoto and T. Tsuzuki, ''Persistent propagation of concentration waves in dissipative media far from thermal equilibrium,'' Prog. Theor. Phys. **55**, 365 (1976).

[36]Y. Kuramoto, *Chemical Oscillations, Waves, and Turbulence* (Springer-Verlag, New York, 1984).

[37]B. Dubrulle and U. Frisch, ''The eddy-viscosity of parity-invariant flow,'' Phys. Rev. A **43**, 5355 (1991).

[38]S. Gama, U. Frisch, and H. Scholl, H. , ''The two-dimensional Navier–Stokes equations with a large-scale instability of the Kuramoto-Sivashinsky type: numerical exploration on the Connection machine,'' J. Sci. Comput. **6**, 425 (1991).

[39]S. Gama, M. Vergassola, and U. Frisch, ''Negative eddy viscosity in isotropically forced two-dimensional flow: Linear and nonlinear dynamics,'' J. Fluid Mech. **260**, 95 (1994).